

# Groundwater salinization in shallow aquifers adjacent to a low-altitude inland salt lake: a case study at Yuncheng Basin, northern China

Chengcheng Li<sup>1</sup> · Tao Liu<sup>1</sup> · Sen Xu<sup>1</sup> · Xubo Gao<sup>1,2</sup> · Yanxin Wang<sup>1</sup>

Received: 16 April 2015 / Accepted: 5 November 2015 / Published online: 23 February 2016  
© Springer-Verlag Berlin Heidelberg 2016

**Abstract** Measurements of chemical composition and environmental isotopes were conducted to investigate the main geochemical processes controlling the salinization of shallow groundwater adjacent to an inland salt lake in the Yuncheng Basin. Hydrogeochemical and isotopic studies were carried out by collecting thirty shallow groundwater, two rainfalls, and one salt lake water samples from the study area. About 80 % of the shallow groundwater samples had total dissolved solids more than 500 mg/L, implying significant water-quality deterioration in the study area. Shallow groundwater showed a clear increased salinity along regional flow paths toward the center of the basin where a salt lake is located. Results of environmental isotopes, ionic ratio, and saturation indices' calculation indicated that the major geochemical processes responsible for groundwater salinization included dissolution of evaporites (halite, gypsum, and mirabilite), cation exchange, and evapotranspiration. Groundwater salinization as a result of salt lake intrusion from the salt lake was limited to the northern shore of the lake.

**Keywords** Groundwater · Salinization · Shallow aquifers · Salt lake · Yuncheng Basin · China

## Introduction

Groundwater salinization has become one of the most acute problems for water resource management worldwide, since it causes deterioration in water quality and endangers future exploitation of groundwater resources. Diverse mechanisms have been proposed for the genesis of groundwater salinization, such as intrusion of seawater into aquifer systems (Barker et al. 1998; Barlow and Reichard 2010), dissolution of evaporites (Rouchy and Caruso 2006; Trabelsi et al. 2007), pollution from oil- and gas-field brine (McMillion 1965), agricultural activities (Wallender and Tanji 1996), concentration by evapotranspiration (Ahmed et al. 2013), saline seepage (Miller 1981), and leakage from wastewater (Ghabayen et al. 2006). Groundwater salinization is aggravated in arid and semi-arid areas, where both anthropogenic activities and natural processes such as water–rock interaction and dissolution of soluble salt in the unsaturated zone accelerate the deterioration of groundwater quality (Houghton et al. 1996; Tanji 1990).

The Yuncheng Basin, located in the southwestern part of Shanxi Province, is a typical semi-arid area in the loess plateau regions of northern China (Han et al. 2006). High TDS concentration groundwater occurrence in the shallow aquifers was reported in numerous studies (Currell et al. 2010; Gao et al. 2007; Yuan 2003). One of the most distinctive geologic features of the basin is the Yuncheng salt lake, a unique low-altitude inland salt lake in China. Intensive groundwater abstraction for industrial, agricultural, and municipal water use for decades has disturbed the dynamic balance between fresh water and saline water, leading to the intrusion of saline water from the salt lake into aquifer systems to degrade basin-scale groundwater quality. Since 1990s, groundwater salinization has been observed in this area, especially in the shallow aquifers

✉ Xubo Gao  
xubo.gao.cug@gmail.com

<sup>1</sup> School of Environmental Studies, State Key Laboratory of Biogeology and Environmental Geology, China University of Geosciences, Postal address: No. 388 Lumo Road, Wuhan 430074, Hubei, China

<sup>2</sup> University of Texas at Austin, Austin, TX 78705, USA

(Chen et al. 1993). However, the processes that control groundwater salinization in the shallow aquifers, which supply groundwater to large population, have been sparsely studied. Our work identifies the possible mechanisms responsible for shallow groundwater salinization in Yuncheng Basin using hydrochemical and stable isotopic ( $\delta^{18}\text{O}$  and  $\delta^2\text{H}$ ) data.

The objective of this study is to integrate hydrological, geochemical, and stable isotope data to reveal the main geochemical processes controlling groundwater salinization in Yuncheng Basin, an arid/semi-arid area. The results of the study can provide a scientific basis for the planning, protection, and decision-making of water resource management in order to prevent the deterioration of water quality and ensure sustainable exploitation of groundwater.

### Geological and hydrogeological settings

The Yuncheng Basin, located between  $34^{\circ}40'$  and  $35^{\circ}30'N$  and  $110^{\circ}15'$  and  $111^{\circ}25'E$ , has an area of  $6211\text{ km}^2$ . Under east-Asian monsoon climatic condition—with the rainy season occurring in July, August, and September and the dry season in November, December, and January—the study area's annual average rainfall is  $550\text{ mm/year}$  (Han et al. 2006), and the pan evaporation is  $1240\text{ mm}$  (Yang and Lu 2005).

Yuncheng Basin is one of the Cenozoic rift basins of the Fenwei Graben in northern China. The Quaternary sediments ( $Q_1$ – $Q_4$ ) are composed of loess, lacustrine silt and clay, and fluvial sand and gravel outcrop in large parts of the basin (Han et al. 2006; Yuncheng Regional Water Bureau and Shanxi province Geological Survey 1982). The unconfined shallow aquifers ( $Q_3$  and locally  $Q_4$ ) are generally 6–20 m thick and distributed in the Sushui River Basin (Figs. 1, 2), occurring at depths less than 70 m below the land surface. Lithologically, the aquifer sediments are gravel and medium-coarse sand in the piedmont plain, medium sand in the alluvial plain, and fine sand in the fluvial depression areas. Bedrock outcrops are Archean metamorphic rocks to the south of the area adjacent to the Zhongtiao Mountain, and composed of hornblende, amphibolite, and quartzite. And the sedimentary rocks, mainly Neogene mudstone and Cambrian-Ordovician limestone, underlie the Quaternary sediments (Yuncheng Regional Water Bureau and Shanxi province Geological Survey 1982).

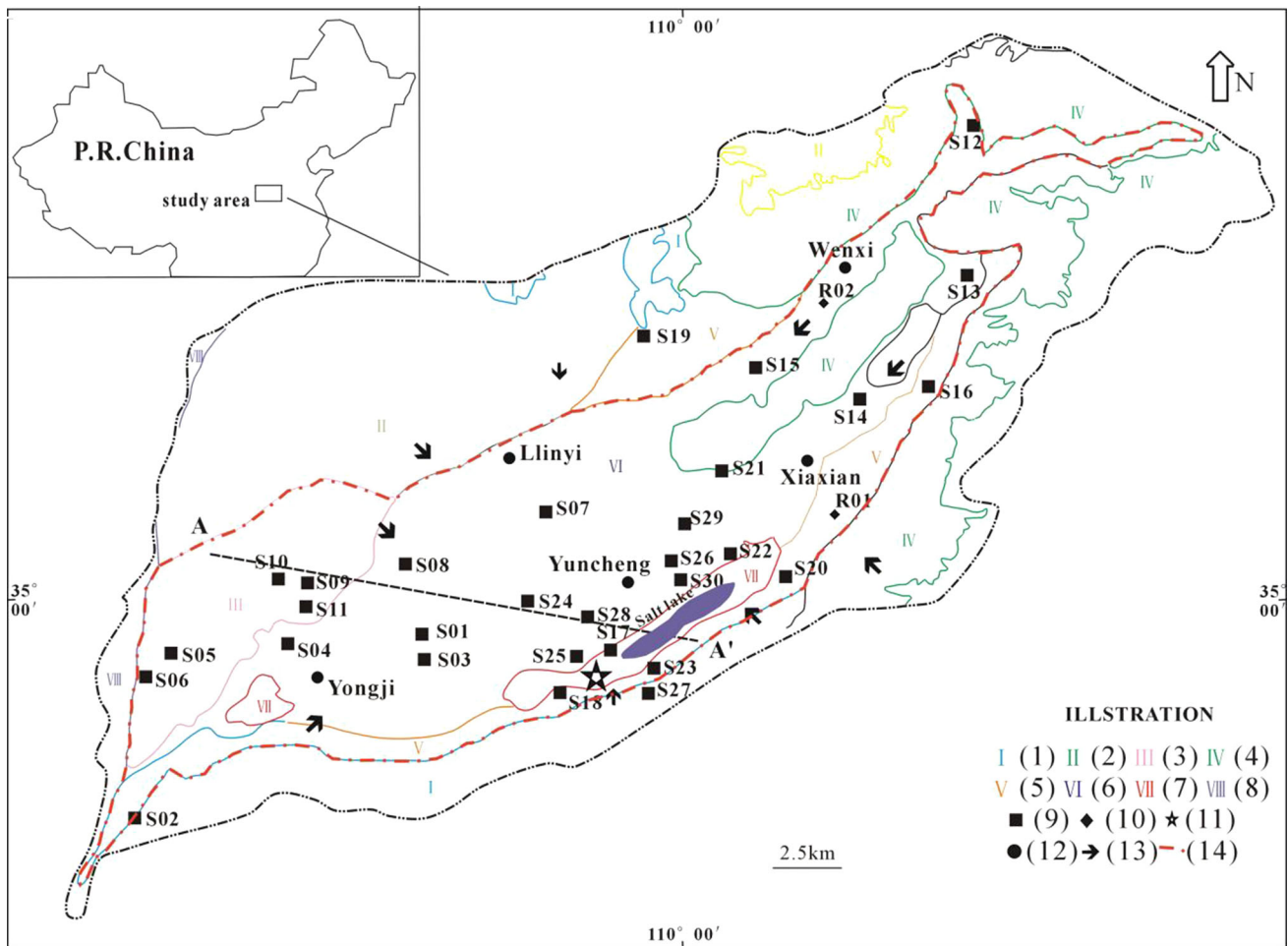
In the basin range, groundwater flows from the margins toward its center. Groundwater is recharged by meteoric water and lateral permeating fissure water along the basin margin, supplemented by leakage of nonperennial river water and irrigation return flow, while discharge occurs via evapotranspiration and artificial abstraction.

### Sampling and analytic methods

The sampling locations for this study are shown in Fig. 1. A total of 33 water samples (thirty shallow groundwater, two rainfalls, and one salt lake water) were collected for hydrochemical and isotopic analyses. The shallow groundwater samples were from shallow aquifers ( $Q_3$  and locally  $Q_4$  aquifers, Fig. 2) wells with depth of 9–70 m in August 2014. Two rainfall samples were collected in July 2011 and we assumed that rainfall hasn't changed its composition between the sampling years. All the water samples were analyzed within 2 weeks after sampling. Hydrochemical data of the rainfalls are presented in Table 1.

Samples for hydrochemical analysis were filtered through  $0.45\text{ }\mu\text{m}$  membranes at the time of sampling and collected in three new 350 mL polyethylene bottles that had been rinsed first with deionized water and then with the sample. Unstable parameters like temperature ( $T$ ), pH and electrical conductivity (EC) were measured in situ using portable Hanna EC and pH meters calibrated before use. Alkalinity was measured on the same day using the Gran titration method. Hydrochemical analyses were performed at the State Key Laboratory of Biological and Environmental Geology, China University of Geosciences. The concentrations of  $\text{Cl}^-$ ,  $\text{SO}_4^{2-}$  and  $\text{NO}_3^-$  were determined using ion chromatography (IC) (Dionex 120, Dionex, Sunnyvale, CA, USA). For cation analysis, reagent-quality  $\text{HNO}_3$  was added to one of these polyethylene bottles until pH of samples was less than 2. Major cations ( $\text{K}^+$ ,  $\text{Na}^+$ ,  $\text{Ca}^{2+}$ , and  $\text{Mg}^{2+}$ ) were measured using inductively coupled plasma-atomic emission spectrometry (ICP-AES) (IRIS Intrepid XSP, Thermo Elemental, Madison, WI, USA). The analytic precision for the measurements of cations and anions was indicated by the ionic balance error, which was observed to be within the standard limit of  $\pm 5\%$ .

Samples for stable isotope analysis ( $\delta^{18}\text{O}$  and  $\delta^2\text{H}$ ) were collected in glass bottles. These bottles were air sealed to avoid fractionation by evaporation, diffusive loss of water vapor, and isotope exchange with the air. Once 100 mL was collected, the samples were stored in a refrigerator at a temperature of approximately  $4\text{ }^{\circ}\text{C}$  till the date of analysis. The  $\delta^{18}\text{O}$  and  $\delta^2\text{H}$  contents of groundwater samples were measured using a Finnigan MAT 253 isotope ratio mass spectrometer at the Institute of Karst Geology, Chinese Academy of Geological Science. All isotopic ratio results were reported using the  $\delta$ -notation as per mill (‰) relative to VSMOW for  $^2\text{H}$  and  $^{18}\text{O}$  standard (IAEA 1993). Samples were measured at least in duplicate, and the precision of the analytic measures were  $\pm 0.1\text{ }‰$  for  $\delta^{18}\text{O}$  and  $\pm 1\text{ }‰$  for  $\delta^2\text{H}$ .



(1) The Bedrock Mountain; (2) The Emei Uplifted Area; (3) The Kaolao Uplifted Area; (4) The Loess Hilly Region; (5) Piedmont Plain; (6) Alluvial Plain; (7) Fluvial Depressions; (8) The Yellow River Terrace; (9) shallow groundwater sampling location; (10) rainfall sampling location; (11) salt lake; (12) country name; (13) horizontal flow direction; (14) Sushui River basin;

Fig. 1 Sampling locations of samples from the Yuncheng Basin, Shanxi Province, China (adapted from Li et al. 2015)

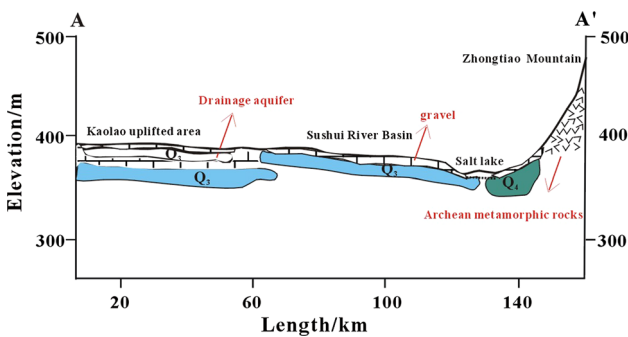


Fig. 2 Schematic cross section A–A' of the shallow aquifers in the basin (the position of cross section is shown in Fig. 1 as A–A'; Adapted from Huang et al., 2007)

## Results and discussion

### Rainfall chemistry

Rainfall is the major source of groundwater recharge in Yuncheng Basin; as a consequence, its quality can have an impact on groundwater chemical composition. Rainfall samples had pH values of 6.24 and 7.08 with total dissolved solids (TDS) of 0.18 and 0.25 g/L, respectively (Table 1). The two samples typically belonged to NaHCO<sub>3</sub> water. An average rainfall composition was calculated based on the data in Table 1, which was used as a broad indication of the chemistry of rainfall/recharge

throughout this study. The assumption was that the rainfall chemistry was not affected by the period during which groundwater in the basin was recharged.

### Groundwater chemistry

The summary of physicochemical parameters, and hydrochemical and stable isotopic compositions of the groundwater samples from Yuncheng Basin is presented in Table 2. Dataset of salt lake water is presented, as one of the possible recharge sources of the shallow aquifers.

Chemistry of the groundwater samples showed wide variations in the concentration ranges. In general, the groundwater samples exhibited pH values within 7.11 and 9.16 (neutral to slightly alkaline). Groundwater temperatures ranged between 15.9 and 23.4 °C influenced by the atmospheric temperature. Sodium was the most abundant cation, with concentrations ranging from 8.3 to 1841 mg/L, followed by  $\text{Ca}^{2+}$  from 4.0 to 124.2 mg/L,  $\text{Mg}^{2+}$  from 4.8 to 349.9 mg/L, and  $\text{K}^+$  from 0.1 to 14.1 mg/L. Moreover, very wide ranges were recognized for anions. The  $\text{Cl}^-$  concentration fluctuated from 19.8 to 1686 mg/L, and  $\text{SO}_4^{2-}$  from 18.5 to 2812 mg/L. Alkalinity, expressed as  $\text{HCO}_3^-$ , was in the range of 148.3–1094 mg/L. Such wide ranges of solute concentrations indicated the effects of a couple of geochemical processes on the water quality. Nitrate concentration was abnormally high (up to 108.3 mg/L) in some groundwater wells, which can be

**Fig. 3** The contour maps of major ions, pH, and TDS values of groundwater samples in Yuncheng Basin. **a**  $\text{Na}^+$ , **b**  $\text{Ca}^{2+}$ , **c**  $\text{Mg}^{2+}$ , **d**  $\text{Cl}^-$ , **e**  $\text{SO}_4^{2-}$ , **f**  $\text{HCO}_3^-$ , **g** pH, **h** TDS (all property values are in mg/L, except for pH, no unit; the arrows represent groundwater horizontal flow direction)

attributed to anthropogenic sources such as agricultural activity, animal wastes, fertilizers, and/or effluents (Heaton 1986). This reflected a considerable risk of aquifer pollution due to nitrate leaching and salinization attributed to human/agriculture activity. The salt lake water exhibited a slightly alkaline pH value (7.95) and an intolerable TDS value (35,150 mg/L). Also, the highest ion concentrations were recorded in this sample.

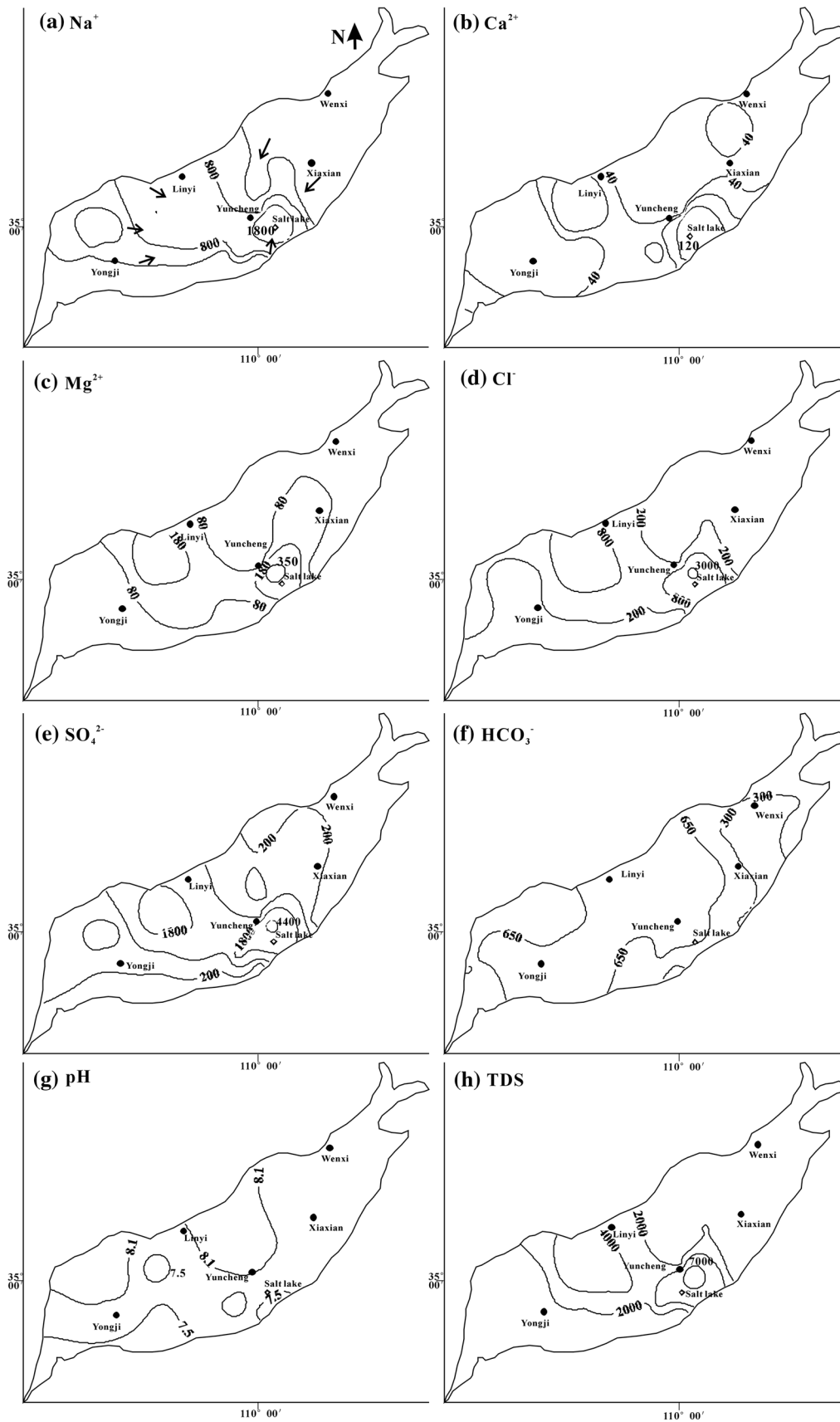
Kriging was chosen for interpolation by means of SURFER software. From the contour maps of major ions, it can be observed that horizontally  $\text{Na}^+$ ,  $\text{Ca}^{2+}$ ,  $\text{Mg}^{2+}$ ,  $\text{Cl}^-$ ,  $\text{SO}_4^{2-}$ ,  $\text{HCO}_3^-$ , pH, and TDS all showed a clear increase along the flow path toward the center of the basin (Fig. 3). This variation agreed well with the general pattern of mineralization evolution of groundwater along the flow path as a result of water–rock interaction. Another interesting finding was that elevated concentrations of ions were also observed near Linyi County. There were two reasons responsible for this. First, in the area near Linyi, the groundwater flow rate was lower. Longer residence time affords more time for the interaction between groundwater and aquifer minerals. This led to increased

**Table 1** Major ion concentrations in rainfall and salt lake samples collected from Yuncheng Basin

Sample ID	Concentrations (mg/L)										(V-SMOW) ‰	
	K	Na	Ca	Mg	Cl	$\text{SO}_4$	$\text{NO}_3$	$\text{HCO}_3$	TDS	pH	$\delta^{18}\text{O}$	$\delta^2\text{H}$
R01	0.4	10.3	3.2	0.4	4.1	5.3	1.2	27	250	6.24	−10.97	−73.8
R02	0.1	7.19	2.6	0.6	3.3	11.5	2.0	17.9	180	7.08	−10.89	−72.7
Average	0.3	8.76	2.9	0.5	3.6	8.4	1.6	22.4	215	6.66	−10.93	−73.3
Salt lake	1014	3760	936	4230	13,008	12,056	20.7	851	35,450	7.95	−5.22	−48

**Table 2** Hydrochemical and isotopic parameters of groundwater samples from the Yuncheng Basin

Parameter	Min	Max	Median	Parameter	Min	Max	Median
T (°C)	15.9	23.4	17.9	$\text{NO}_3$ (mg/L)	3.1	108	14
pH	7.1	9.2	7.9	$\text{HCO}_3$ (mg/L)	148	1094	554
Depth	9	70	30	Br ( $\mu\text{g/L}$ )	52.2	5250	379
TDS (g/L)	0.28	7.10	1.04	$\delta^{18}\text{O}$ (‰)	−10.4	−6.4	−8.3
K (mg/L)	0.1	14.1	1.8	$\delta^2\text{H}$ (‰)	−76.9	−53	−62.7
Na (mg/L)	8.3	1841	284	$\text{SI}_{\text{halite}}$	−7.7	−3.5	−3.5
Ca (mg/L)	4.0	124	33.6	$\text{SI}_{\text{gypsum}}$	−3.4	−0.3	−1.7
Mg (mg/L)	4.8	350	45.8	$\text{SI}_{\text{calcite}}$	−0.2	0.8	0.2
Cl (mg/L)	19.8	1686	153	$\text{SI}_{\text{dolomite}}$	0.2	2.2	1.2
$\text{SO}_4$ (mg/L)	18.5	2812	295				





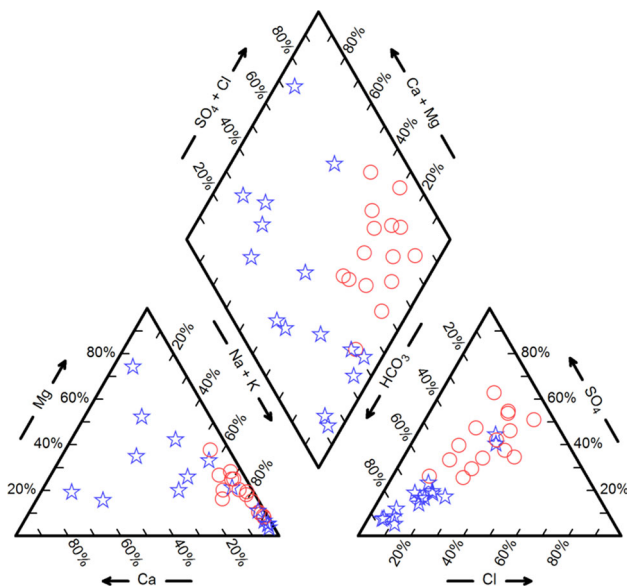


**Fig. 4** Piper diagram showing the hydrochemical facies of the shallow groundwater in the Yuncheng Basin. Legend: *star* groundwater samples with TDS <1000 mg/L, *circle* groundwater samples with TDS >1000 mg/L

concentrations of most ions in groundwater. In addition, ion exchange was another factor leading to the elevated ions' concentration in the groundwater near Linyi. Over 50 % of groundwater samples collected fell under brackish or saline water category according to the classification of Freeze and Cherry (1979) with TDS values ranging from 280 to 17,450 mg/L. Groundwater with low TDS values was typical  $\text{HCO}_3$  type water, while high-TDS groundwater normally belonged to  $\text{SO}_4$ -Cl and  $\text{HCO}_3$ - $\text{SO}_4$ -Cl types (Fig. 4). The comparison of the hydrochemical data with the United States Environmental Protection Agency (USEPA) drinking-water standards showed that about 80 % ( $n = 24$ ) of the groundwater samples exceeded the guidance values for TDS (500 mg/L), 37 % ( $n = 11$ ) for chloride (250 mg/L), and 6 % ( $n = 2$ ) for nitrate (44.3 mg/L), reflecting the significant water-quality deterioration in the study area.

### Environmental isotopes

The isotopic variations of oxygen and hydrogen have been widely applied to assess the genesis and evolution of groundwater, to understand the mixing and evaporation effects, and to provide clues about the salinity sources that affect the quality of groundwater.

Stable isotopic composition of the analyzed groundwater samples ranged from  $-9.4$  to  $-7.38$  ‰ for  $^{18}\text{O}$  and from  $-70.6$  to  $-59.3$  ‰ for  $^2\text{H}$ , respectively. The standard diagram of  $\delta^{18}\text{O}/\delta^2\text{H}$  (Fig. 5) shows the position of all samples relative to the global meteoric water line (GMWL:  $\delta^2\text{H} = 8\delta^{18}\text{O} + 10$ ; Craig 1961) and local meteoric water line (LMWL:  $\delta^2\text{H} = 7.1\delta^{18}\text{O} + 4.8$ ; International Atomic Energy Agency/World Meteorological Organization 2007).

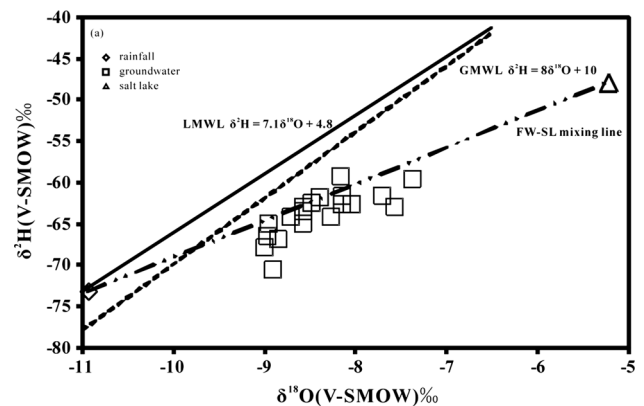


**Fig. 5**  $\delta^{18}\text{O}$  vs.  $\delta^2\text{H}$  plot of the groundwater samples from the Yuncheng Basin compared with the GMWL and LMWL

$\delta^2\text{H} = 8\delta^{18}\text{O} + 10$ ; Craig 1961) and local meteoric water line (LMWL:  $\delta^2\text{H} = 7.1\delta^{18}\text{O} + 4.8$ ; International Atomic Energy Agency/World Meteorological Organization 2007). The mean values of  $\delta^{18}\text{O}$  and  $\delta^2\text{H}$  for rainfall samples as well as salt lake water were also presented as potential recharge sources. The rainfall sample fell on the GMWL and LMWL lines and was isotopically depleted. The salt lake sample was distinctly enriched in its stable isotopic compositions by  $-5.22$  ‰ for  $^{18}\text{O}$  and  $-48$  ‰ for  $^2\text{H}$ . On the  $\delta^{18}\text{O}$  vs.  $\delta^2\text{H}$  plot, all groundwater samples fell close to the GMWL and LMWL line, indicating a precipitation origin of groundwater in this area. This diagram showed that all groundwater samples were located right to the MWL. Gibson et al. (1993) revealed that groundwater that had undergone evaporation displayed systematic enrichment of  $^{18}\text{O}$  and  $^2\text{H}$ , which resulted in the divergence from the GMWL along the evaporation lines that had slopes of less than 8. As a consequence, deviation from the slope of eight in shallow groundwater in Yuncheng Basin was the characteristic of water subject to evaporation through a dry surface layer due to non-equilibrium isotope fractionation under the low moisture condition. It was also noticed that a few groundwater samples lay more or less on the straight line connecting the isotopic compositions of rainfall and salt lake end-members, as shown in Fig. 5. This can be regarded as a sign of the possibility of salt lake intrusion which was previously reported by others (Gao et al. 2007; Khair et al. 2014; Li et al. 2015).

### Chemical components in groundwater

#### Correlation between individual chemical components and salinization (TDS)

Mixing and chemical reactions, such as ion-exchange, dissolution-precipitation, evapotranspiration processes,

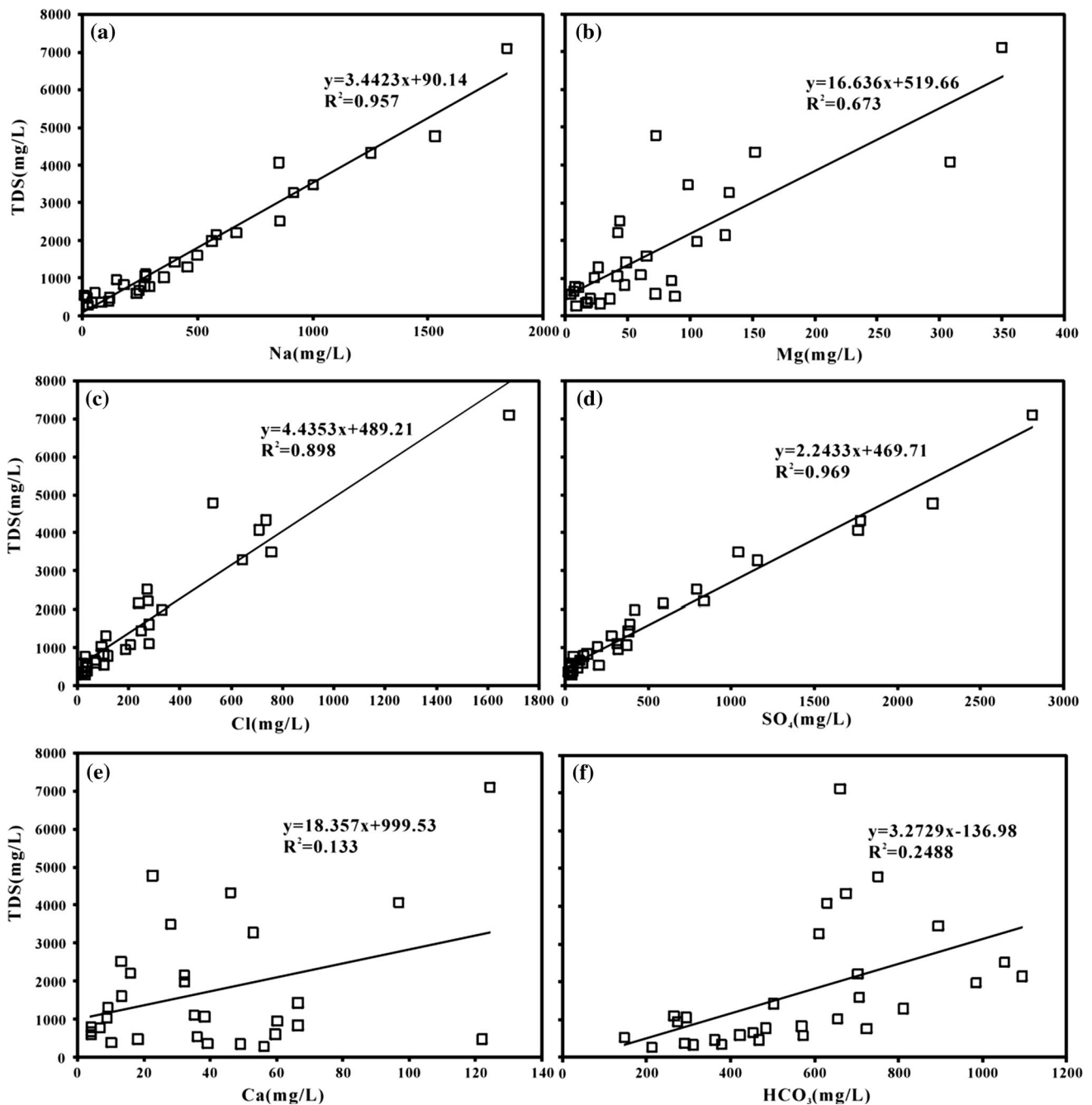


**Fig. 6** Scatter maps between major ion concentrations (hydrochemical parameter) and TDS in groundwater: **a** Na<sup>+</sup>, **b** Mg<sup>2+</sup>, **c** Cl<sup>-</sup>, **d** SO<sub>4</sub><sup>2-</sup>, **e** Ca<sup>2+</sup>, **f** HCO<sub>3</sub><sup>-</sup>

and salt lake intrusion are potential processes controlling groundwater chemistry at Yuncheng Basin (Li et al. 2015). To obtain source information about the chemical composition of groundwater in the Yuncheng Basin, composition diagrams were applied in this study. These diagrams show major ions' (Na<sup>+</sup>, Mg<sup>2+</sup>, Cl<sup>-</sup>, SO<sub>4</sub><sup>2-</sup>, Ca<sup>2+</sup>, and HCO<sub>3</sub><sup>-</sup>) concentrations against TDS value. There was a well-defined linear correlation between Na<sup>+</sup>, Mg<sup>2+</sup>, Cl<sup>-</sup>, and

SO<sub>4</sub><sup>2-</sup> with TDS, as shown in Fig. 6, indicating the positive contribution of these components to groundwater salinity. Na<sup>+</sup>, Cl<sup>-</sup>, and SO<sub>4</sub><sup>2-</sup> were found in larger amounts in the subsurface sediments as evaporites such as halite (NaCl), mirabilite (Na<sub>2</sub>SO<sub>4</sub>·10H<sub>2</sub>O), and gypsum (CaSO<sub>4</sub>·2H<sub>2</sub>O) at Yuncheng (Han et al. 2006). The observed well-defined correlation between TDS and Na<sup>+</sup> ( $R^2 = 0.957$ ,  $p = 0.01$ ), Cl<sup>-</sup> ( $R^2 = 0.898$ ,  $p = 0.01$ ), and SO<sub>4</sub><sup>2-</sup> ( $R^2 = 0.969$ ,

$p = 0.01$ ) and the abnormally high contents of these major elements in shallow groundwater suggested that the leaching dissolution of evaporites was one of the main factors that affected the groundwater chemistry. The low observed correlation between TDS and  $\text{Ca}^{2+}$  ( $R^2 = 0.133$ ,  $p = 0.01$ ; Fig. 6e) could be related to cation-exchange processes between  $\text{Na}^+$  and  $\text{Ca}^{2+}$  and/or carbonate precipitation (Guo and Wang 2005). An insignificant correlation between  $\text{HCO}_3^-$  and TDS concentrations (Fig. 6f) was observed. The major source of  $\text{HCO}_3^-$  was mineral weathering dissolution in natural groundwater at Yuncheng. The low correlation between  $\text{HCO}_3^-$  and TDS concentrations indicated that bicarbonate in shallow groundwater was seriously modified by other geochemical processes, e.g., calcite and dolomite precipitation formation (Wang et al. 2009).

#### Sources of major ions in groundwater

**Sources of sodium, chloride, and sulfate** The stoichiometric relations among dissolved species are introduced for the further determination of sources of major ions in the shallow groundwater (Fig. 7). The Na–Cl relationship had often been used to understand the mechanisms of groundwater acquiring salinity in semi-arid/arid regions (Sami 1992). Sodium displayed positive correlation with chloride with  $R^2 = 0.792$  (Fig. 7a). Groundwater samples with low  $\text{Na}^+$  and  $\text{Cl}^-$  concentration were placed along the halite dissolution line characterized by a slope of 1.0, illustrating the dissolution source of  $\text{Na}^+$  and  $\text{Cl}^-$  from halite in the fresh water. However, block of groundwater samples were positioned above the halite dissolution line which can't be simply interpreted by halite dissolution (Appelo and Postma 1993). The enrichment of  $\text{Na}^+$  relative to  $\text{Cl}^-$  gave clues regarding the contribution of other processes such as cation exchange or the dissolution of other sodium salts to the groundwater mineralization.

Another possible source of  $\text{Na}^+$  in groundwater was sodium obtained via cation exchange. A phenomenological evidence for cation exchange was provided by bivariate diagram of  $(\text{Ca}^{2+} + \text{Mg}^{2+}) - (\text{HCO}_3^- + \text{SO}_4^{2-})$  as a function of  $(\text{Na}^+ - \text{Cl}^-)$  (unit in meq/L) (Fig. 7b). The  $(\text{Na}^+ - \text{Cl}^-)$  represented the amount of  $\text{Na}^+$  gained or lost relative to that provided by calcite, dolomite, and gypsum dissolution, whereas  $(\text{Ca}^{2+} + \text{Mg}^{2+}) - (\text{HCO}_3^- + \text{SO}_4^{2-})$  provided the sum of the cations of Ca and Mg from sources other than their respective carbonates and sulfates. If cation exchange was an important factor controlling groundwater chemistry, the samples would fall around a 1:1 straight line on the plot. In the absence of these reactions in significant quantities to influence the hydrochemistry, all points should be close to the origin (Jalali 2007). Figure 7b shows

all groundwater samples that were plotted around a straight line with the slope of  $-1.002$  and  $R^2 = 0.99$ , which stood for cation exchange as a major process controlling the chemistry of shallow groundwater at Yuncheng Basin. It was also noticed that most samples exhibited an increase in  $\text{Na}^+$  with a decrease in  $(\text{Ca}^{2+} + \text{Mg}^{2+})$  or an increase in  $(\text{HCO}_3^- + \text{SO}_4^{2-})$  concentration. This implied that the cation-exchange sites preferentially adsorbed  $\text{Ca}^{2+}$  and  $\text{Mg}^{2+}$  and released  $\text{Na}^+$  to the aqueous phase.

Dissolution of evaporites is another source of  $\text{Na}^+$  and also  $\text{Cl}^-$ ,  $\text{SO}_4^{2-}$  in shallow groundwater. In the central basin area, groundwater flows slower, and thus greater evapotranspiration rates can be expected in the unsaturated zone (Carol et al. 2009; Li et al. 2015). Strong evapotranspiration has led to the accumulation of evaporites, such as mirabilite, gypsum, and halite in sediment in this semi-arid area. The Quaternary sediments at Yuncheng Basin are composed of aeolian loess, lacustrine clays, fluvial sands, and gravels, mixed with mirabilite and gypsum (Han et al. 2006; Wang et al. 2013). These groups are susceptible for weathering dissolution. The vertical recharge by irrigation returns and salt-flushing water can bring more sodium, sulfate, and chloride into the shallow groundwater via dissolving evaporites. On the bivariate plots, TDS showed a high positive correlation with  $\text{Na}^+$ ,  $\text{SO}_4^{2-}$ , and  $\text{Cl}^-$ , and a moderate correlation with  $\text{Ca}^{2+}$  (Fig. 6), which proposed the potential contribution of widely distributed evaporites in sediments to groundwater chemistry. A graph of  $\text{SO}_4^{2-}$  vs.  $\text{Na}^+ - \text{Cl}^-$  concentration (mmol/L) may denote the contribution of evaporites dissolution to groundwater sodium and sulfate (Fig. 8). According to the variation of  $\text{Na}^+ - \text{Cl}^-$  concentration, the groundwater chemistry evolution was divided into two stages, along the increase of sulfate content. In the first stage, increasing sulfate content in groundwater was accompanied by a gradual elevation of  $\text{Na}^+ - \text{Cl}^-$  content. This elevated  $\text{Na}^+ - \text{Cl}^-$  content could be explained by cation exchange which we mentioned before. Along the flow path, cation exchange occurred between groundwater and the aquifer sediments where:  $\text{Ca}^{2+}$  and  $\text{Mg}^{2+}$  were adsorbed onto and  $\text{Na}^+$  was desorbed from the clay matrix. In the second stage, a rapid increase of  $\text{Na}^+ - \text{Cl}^-$  concentration was observed which was entirely different from the first stage where cation exchange acted as a major factor on groundwater sodium. Dissolution of sulfate evaporites was supposed to be the major source of sodium and sulfate in this stage. According to the reports from others and our group (Currell et al. 2010; Han et al. 2006; Gao et al. 2007; Wang et al. 2013; Li et al. 2015), main sources of sodium in groundwater included weathering of silicate rocks, cation exchange, and sodium salt dissolution (mainly halite and mirabilite) in this area. A mass of sodium input in this stage could only be attributed to the dissolution of sodium sulfate.



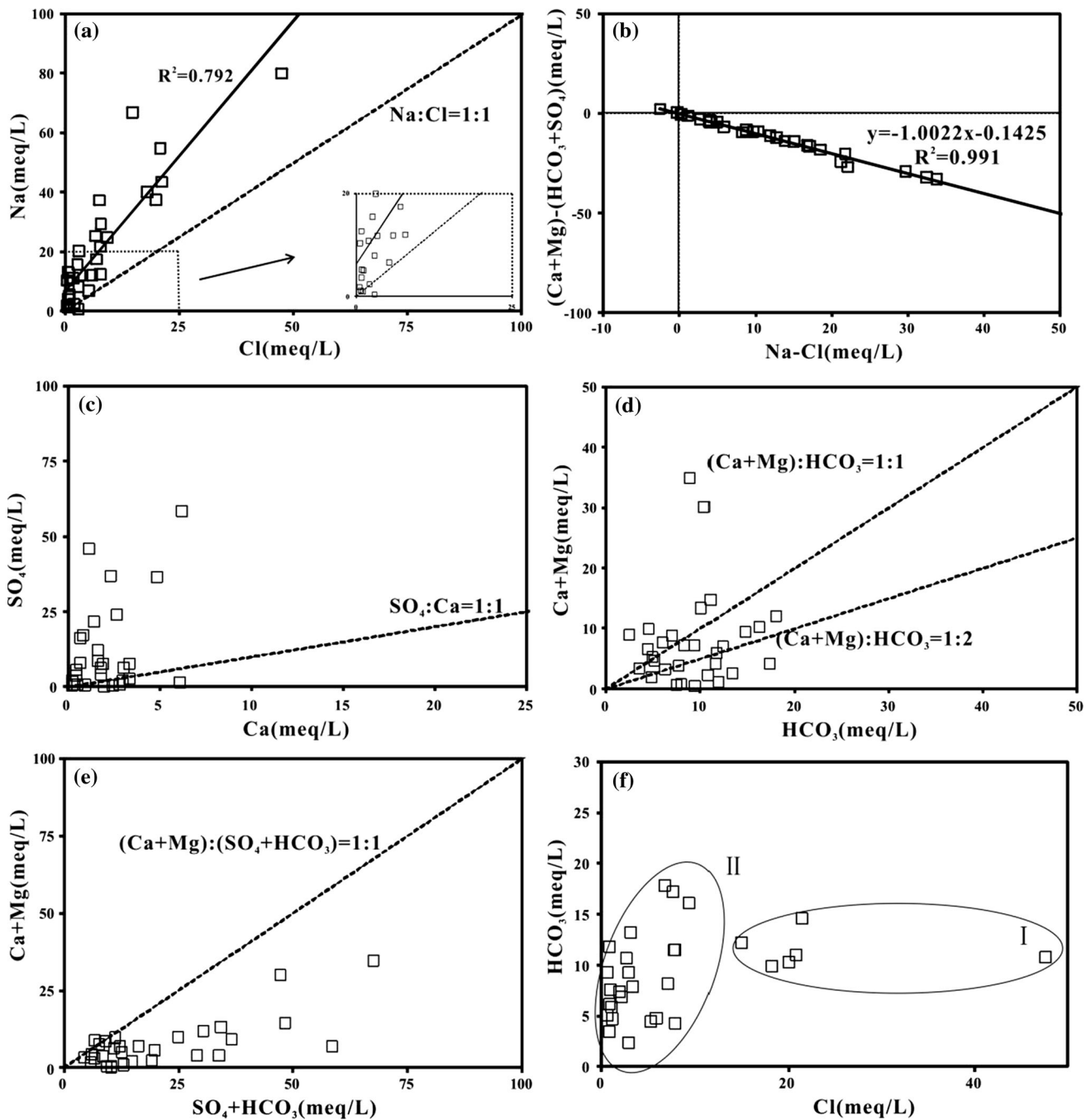
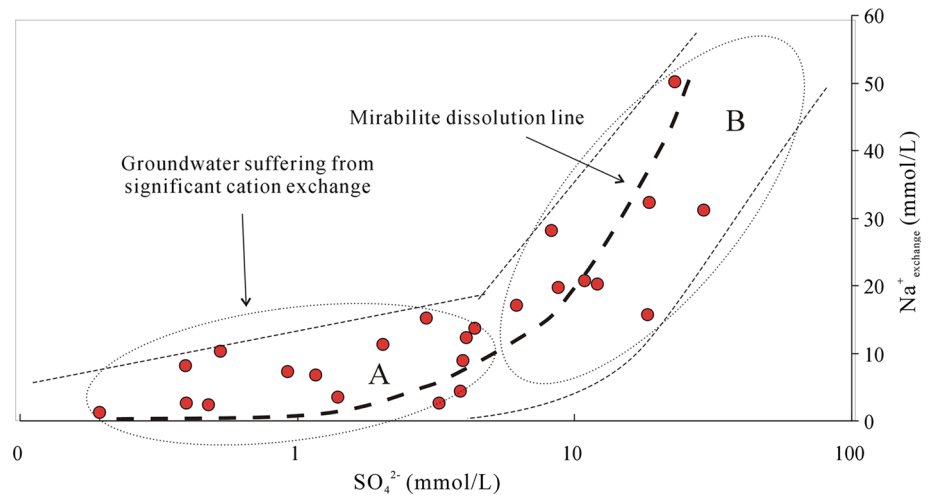


Fig. 7 Relationships between major ions for groundwater samples

Most of groundwater samples lying on or close to the mirabilite dissolution line suggested the major contribution at this stage. Some groundwater samples lay over the dissolution line reflecting the action of cation exchange at this stage. Samples stayed on the right of the mirabilite dissolution line suggesting an additional source of sulfate which was moderately conducted as gypsum, the only possible remaining source of sulfate in the area.

*Sources of calcium and magnesium* Understanding calcium content variation is important for us to identify some specific processes involved in the groundwater chemistry. From Fig. 7c, it can be seen that most groundwater samples had  $Ca^{2+}/SO_4^{2-}$  ratio less than 1.0. The excess of  $SO_4^{2-}$  with respect to  $Ca^{2+}$  reflected that, in addition to gypsum dissolution, there should be extra sources of  $SO_4^{2-}$  and/or a deficit of  $Ca^{2+}$ . Cation exchange tended to remove some

**Fig. 8** Bivariate diagram of  $\text{Na}^+_{\text{exchange}}$  as a function of  $\text{SO}_4^{2-}$  (unit in mmol/L). In the group A (water samples from the flow-through area), the  $\text{Na}^+_{\text{exchange}}$  value represents the sodium obtained from cation exchange; in the group B (groundwater samples from discharge area with bulk evaporites dissolution), the value represents the sodium obtained by cation exchange and evaporites (mainly mirabilite) dissolution



calcium from water into clay mineral matrix. Besides, precipitations of calcite and dolomite may be another causative factor responsible for the removal of  $\text{Ca}^{2+}$  from the aqueous phase. The saturation indices of groundwater samples were calculated and are listed in Table 2. Groundwater samples collected from the recharge areas (No. S02, S12, S16, S18, S20, S23, and S27) normally had a negative  $\text{SI}_{\text{calcite}}$  value demonstrating their potential ability in calcite dissolution. On the contrary, groundwater samples from the flow-through areas and discharge areas displayed the precipitation tendencies of calcite and dolomite with the high positive  $\text{SI}_{\text{calcite}}$  and  $\text{SI}_{\text{dolomite}}$  values.

A  $(\text{Ca}^{2+} + \text{Mg}^{2+})/\text{HCO}_3^-$  ratio can give additional information for the sources of  $\text{Ca}^{2+}$  and  $\text{Mg}^{2+}$  in groundwater. If  $\text{Ca}^{2+}$  and  $\text{Mg}^{2+}$  in groundwater only originate from the dissolution of carbonates in the aquifer materials and from the weathering of accessory pyroxene or amphibole minerals, this ratio would be about 0.5 (Sami 1992). As shown in Fig. 7d, parts of the groundwater samples fell around the line with  $(\text{Ca}^{2+} + \text{Mg}^{2+})/\text{HCO}_3^-$  ratio being equal to 0.5, while a block of data points fell above the 1:2 and 1:1 trend line reflecting the extra sources for recharge of  $\text{Ca}^{2+}$  and  $\text{Mg}^{2+}$  in groundwater. Based on the field and indoor mineralogical investigations by others and our group (Han et al. 2006; Li et al. 2015; Wang et al. 2013), gypsum was considered as one of the most reliable mineral sources for this additional  $\text{Ca}^{2+}$  input. To evaluate the contribution of gypsum and carbonate minerals' dissolution to groundwater calcium chemistry, correlation between  $(\text{Ca}^{2+} + \text{Mg}^{2+})$  with respect to  $(\text{HCO}_3^- + \text{SO}_4^{2-})$  is presented in Fig. 7e. In this figure, data points falling along and below the 1:1 equilibrium line suggested that these ions had either resulted from or been dominantly affected by weathering dissolution of calcite, dolomite, and gypsum (Datta and Tyagi 1996). Those that fell above the

1:1 line reflected the requirement of cations from reverse cation exchange and/or weathering of silicate rocks. As seen in Fig. 7e, all the groundwater samples fall around and below the 1:1 line, indicating the contributions from carbonate and gypsum dissolution. Besides, most of the points showed a deficiency of  $(\text{Ca}^{2+} + \text{Mg}^{2+})$  relative to  $(\text{HCO}_3^- + \text{SO}_4^{2-})$ . Therefore, the excess negative charges of  $\text{SO}_4^{2-}$  and  $\text{HCO}_3^-$  must be balanced by  $\text{Na}^+$ , the only other major cation.

*Influence of salt lake intrusion on groundwater chemistry* A graph of bicarbonate and chloride (Fig. 7f) shows a way to distinguish the influence of salt lake intrusion on shallow groundwater chemistry. Groundwater samples were separated into two groups: (1) moderate-to-high  $\text{Cl}^-$  content and moderate  $\text{HCO}_3^-$  content; and (2) low  $\text{Cl}^-$  content and varied  $\text{HCO}_3^-$  content. The significant elevation of  $\text{Cl}^-$  content in group 1, led us to believe that groundwater there was suffering from salt lake water intrusion, since the salt lake water was characterized as high  $\text{Cl}^-$  (13,008 mg/L),  $\text{SO}_4^{2-}$  (12,056 mg/L) and  $\text{Na}^+$  (3760 mg/L) content. The moderate bicarbonate contents embodied the combined action of minerals' dissolution and precipitation on chemistry in the above groundwater. During the evolution of groundwater from recharge areas to discharge areas, it obtained bicarbonate from carbonates and silicate minerals' dissolution. However, mixing with salt lake water tended to remove bicarbonate from groundwater via carbonates' precipitation. It could be explained by the theory of common ion effect. Fast loading of  $\text{Ca}^{2+}$  and  $\text{Mg}^{2+}$  from salt lake water may result in the oversaturations of carbonate and dolomite. Thus, the concentration of groundwater bicarbonate would be reduced via the precipitation of these minerals. Groundwater from group 2 had varied bicarbonate contents and

low-to-medium Cl<sup>-</sup> concentrations. It could be the result of water–rock interaction along the groundwater flow paths.

**Salinization processes**

*Quantifying salt lake intrusion*

To quantify the mixing ratios of salt lake water and fresh water in the investigated system, we considered the chloride balance. It was assumed that Cl<sup>-</sup> was a conservative tracer (Tellam 1995) and that the balance has not been affected by halite dissolution. The following mass balance equation was used (Appelo and Postma 2005):

$$F = \frac{[Cl_{sample}^-] - [Cl_{fresh}^-]}{[Cl_{sl}^-] - [Cl_{fresh}^-]} \times 100 \tag{1}$$

where *F* is the percentage of salt lake contribution to groundwater chemistry; Cl<sup>-</sup><sub>sample</sub> is the chloride concentration in possible affected groundwater; Cl<sup>-</sup><sub>fresh</sub> is the chloride concentration in the upstream non-affected groundwater; and Cl<sup>-</sup><sub>sl</sub> is the chloride concentration of salt lake.

The calculated values of salt lake contribution varied from 0.07 to 4.27 % (Table 3). This suggested that the effect of salt lake on groundwater salinization was not widely distributed in the area. The highest values were found in the northern shore groundwater, indicating that the northern part close to the salt lake was the area most seriously affected by salt lake intrusion.

*Water–rock interaction*

Salt lake intrusion is not the only process that determines the salinization of waters. Indeed, water-weathering rock interaction has been found to be another main factor

controlling groundwater salinization. In this case study, effects of water–rock interactions on groundwater salinization were investigated by calculating minerals saturation indices for groundwater samples (Table 2) using PHREEQC (Parkhurst and Appelo 1999). Using the saturation index (SI) approach, it is possible to predict the subsurface mineralogy from groundwater data without collecting the samples of the solid phase and analyzing the mineralogy (Deutsch 1997). If the groundwater is saturated with respect to a mineral (SI > 0), it is of potential to precipitate this mineral phase out of solution. Although if it is under-saturated (SI < 0), it will continue to dissolve. Figure 9 shows the variation trends of the minerals saturation indices with groundwater TDS. The results showed that groundwater was unsaturated or slightly saturated with respect to calcite and dolomite and, unsaturated with respect to halite and gypsum in the low TDS areas. The saturation indices of calcite, dolomite, halite, and gypsum increased in steps as the TDS increased, illustrating the major involvement of dissolution of carbonates and salt minerals. Along the groundwater flow direction, the presence of cation exchange would remove Ca<sup>2+</sup> and Mg<sup>2+</sup> from the groundwater. In this case, the increased SI values of calcite and dolomite represented the dissolution of other calcium- and/or magnesium-bearing minerals, e.g., gypsum. This is due to the fact that the dissolution of gypsum could lead to the increase of Ca<sup>2+</sup> concentration in groundwater. Elevated Ca<sup>2+</sup> concentration would further enhance the oversaturation status of calcite, and promote its precipitation. Elevation of Ca<sup>2+</sup> concentration in groundwater would also intensify the oversaturation status of dolomite. However, dolomite was hard to be removed from groundwater via precipitation, compared with calcite. As a result, high content of Mg<sup>2+</sup> remained in groundwater during salinization. Magnesium-bearing minerals were not

**Table 3** Groundwater chemistry and calculated percentage of salt lake contribution

Water samples	K <sup>+</sup>	Na <sup>+</sup>	Ca <sup>2+</sup>	Mg <sup>2+</sup>	Cl <sup>-</sup>	SO <sub>4</sub> <sup>2-</sup>	HCO <sub>3</sub> <sup>-</sup>	F (%)
North shore upstream fresh groundwater								
S29	0.1	353.7	8.6	23.5	93.1	194.5	654.7	–
North shore groundwater								
S17	1.7	1530	22.4	73.0	529.2	2213	750.5	3.38
S28	1.8	916.8	52.9	131.7	644.5	1159	609.9	4.27
S30	0.4	562	32.1	105.6	330.6	419.7	984.1	1.84
South shore upstream fresh water								
S27	3.4	25.8	56.1	9.0	27.6	41.0	213.1	–
South shore groundwater								
S18	4.4	54.6	59.5	72.5	73.3	104.1	422.5	0.35
S23	3.8	21.6	121.8	20.4	37.2	78.0	363.0	0.07
Salt lake water	1014	3760	936.0	4230	13,008	12,056	851.0	–

All the ions are measured in mg/L

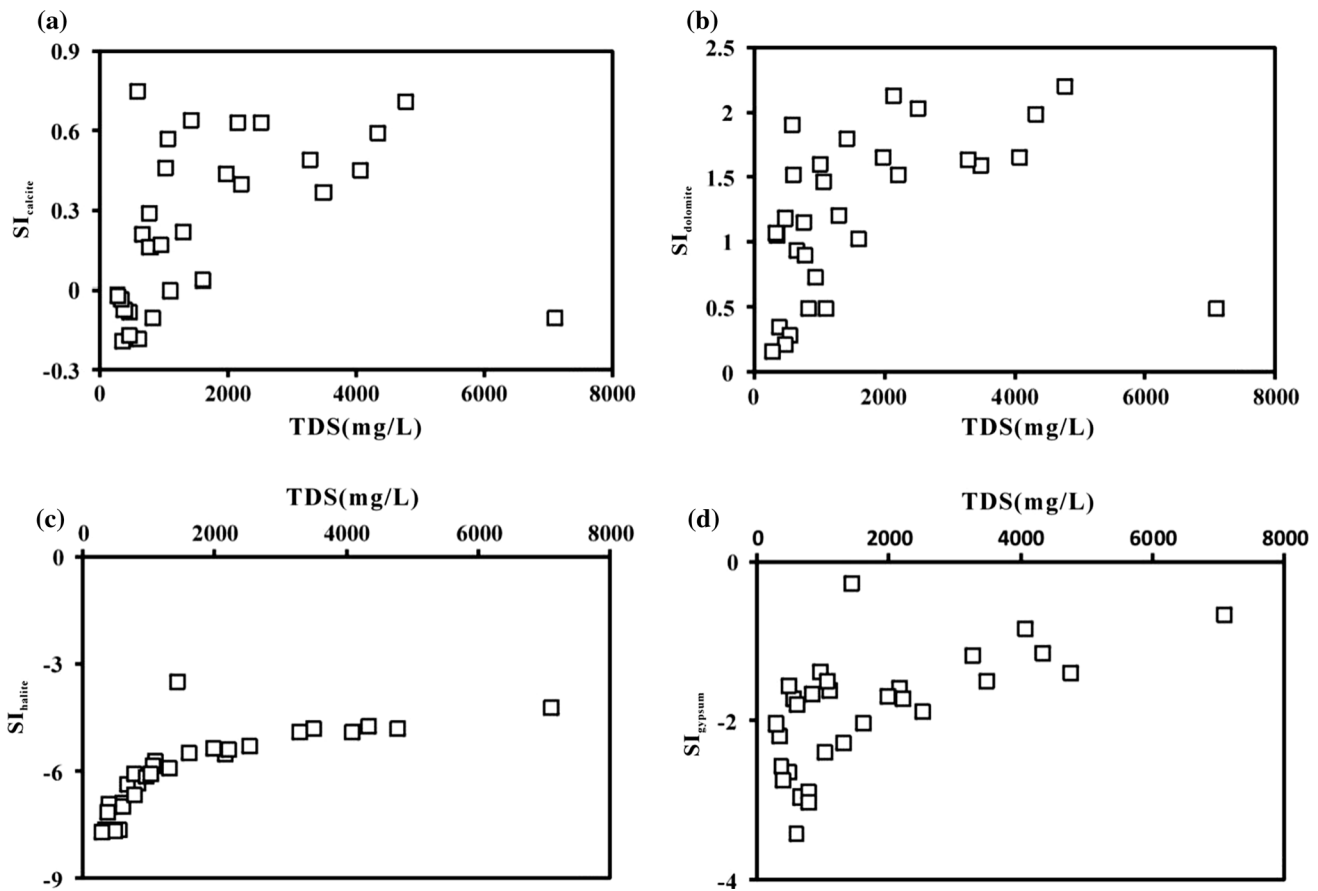


**Fig. 9** Scatter maps of TDS and four major minerals saturation index in groundwater (**a** calcite, **b** dolomite, **c** halite, and **d** gypsum)

found in Quaternary sediments in the area. Their contribution to groundwater salinization was not taken into consideration. Dissolution of halite occurred throughout the whole process of groundwater chemistry evolution. Based on the minor amount of anthropogenic chloride input, halite dissolution was considered as the only major source of  $\text{Cl}^-$  in groundwater. Dissolution of other salt minerals, e.g., mirabilite, also made a significant contribution to groundwater salinization.

#### Cation exchange

Cation-exchange reactions are also important for groundwater salinization (Appelo and Greinaert 1991; Cruz and Silva 2000). Ion exchange reactions often occur when a certain amount of clay type sediment is placed in contact with a solution that contains an excess of a given cation. In this case study, ion exchange happened during groundwater flowing from recharge area to discharge area, and saline water mixing with fresh groundwater. It was of significance to quantify the contribution of cation exchange to groundwater salinization. The contribution of cation exchange to groundwater salinization was evaluated using

the sodium concentration variation in the groundwater. The sodium concentration elevation due to cation exchange in the flow-through area can be expressed as

$$\text{Na}_{\text{exchange}} = \text{Na}_{\text{total}} - \text{Na}_{\text{initial}} - \text{Na}_{\text{dissolved}} \quad (2)$$

where  $\text{Na}_{\text{exchange}}$  is the sodium obtained from cation exchange;  $\text{Na}_{\text{total}}$  is the total sodium in groundwater; and  $\text{Na}_{\text{initial}}$  is the initial sodium concentration (average sodium concentration in upstream groundwater, ca. 1.0–2.0 mmol/L in this case study, data not shown);  $\text{Na}_{\text{dissolved}}$  is the mineral dissolution sodium obtained along the flow path (we assumed that it was mainly from halite; the contribution of other minerals was ignored due to the short distance and contact time), and it was represented by  $\text{Cl}^-$  concentration in groundwater. Therefore, the  $\text{Na}_{\text{exchange}}$  value could represent the sodium obtained from cation exchange in the flow-through area (Fig. 8, group A) where the contribution of mirabilite to groundwater chemistry was insignificant. However, in the group B (groundwater from discharge area with bulk evaporites dissolution), the value  $\text{Na}_{\text{exchange}}$  represented the sodium obtained by both cation exchange and evaporites (mainly mirabilite) dissolution.

Figure 8 also shows an increase in  $\text{Na}_{\text{exchange}}$  concentration in the flow-through area (group A), along with the increase of sulfate from the recharge area to the flow-through area. This value was calculated using the Eq. (2). Therefore, it can be an estimation of sodium obtained from cation exchange in the recharge and flow-through area. The contribution of cation exchange to groundwater salinization (in  $\text{Na}^+$  concentration) was estimated to be 1.23–15.20 mmol/L in this stage. Also, many groundwater samples dropped close to the mirabilite dissolution line (Fig. 8, group B), which further confirmed the contribution of mirabilite dissolution to groundwater salinization in the area. Moreover, the contribution of mirabilite dissolution was estimated up to 50.2 mmol/L  $\text{Na}^+$  to groundwater chemistry (Fig. 8, data not shown).

### Evapotranspiration

Salts could be concentrated in the subsurface shallow groundwater due to the pan evaporation rates that exceed precipitation by one order of magnitude, especially in the arid/semi-arid basin (Geraghty and Miller 1973). The Yuncheng Basin is a typical semi-arid area with the pan evaporation far exceeding the annual precipitation. Under such conditions, evapotranspiration (either during recharge or from shallow water tables) enriches ion concentrations in shallow groundwater. This effect of evapotranspiration is more intensified when it comes to the center of the basin where groundwater moves slowly in the fine sand, silt, and clay. Evapotranspiration from groundwater table could be evidenced from the deviations in isotope compositions of groundwater (Fig. 5).

### Conclusions

Integrated analysis of hydrochemical and environmental isotopic data provide important clues for understanding the main processes controlling shallow groundwater salinization at Yuncheng.

1. Salt lake intrusion has affected the water quality of wells located near the salt lake. The calculated percentage of salt lake intrusion in the groundwater samples indicates that the effect of salt lake is more pronounced in the northern part close to the salt lake where the percentage reaches up to 4.27 %.
2. Water–rock interaction including dissolution of halite, gypsum, and mirabilite, and evapotranspiration have an impact on groundwater salinization, as indicated by hydrochemistry and stable isotopic composition data and saturation indices.

3. Cation-exchange reactions result in enrichment in  $\text{Na}^+$  content and depletion in  $\text{Ca}^{2+}$  and  $\text{Mg}^{2+}$  concentrations in groundwater at the recharge and flow-through area. The contribution of cation exchange to groundwater salinization (in  $\text{Na}^+$  concentration) is estimated to be 1.23–15.20 mmol/L in these areas.

**Acknowledgments** The research work was financially supported by the National Natural Science Foundation of China (No. 41120124003 and No. 41372251), the Ministry of Science and Technology of China (2012AA062602), China Geological Survey (No. 1212011220949), and the International Postdoctoral Exchange Fellowship Program by the Office of China Postdoctoral Council.

### References

- Ahmed MA, Samie SGA, Badawy HA (2013) Factors controlling mechanisms of groundwater salinization and hydrogeochemical processes in the Quaternary aquifer of the Eastern Nile Delta, Egypt. *Environ Earth Sci* 68(2):369–394
- Appelo CAJ, Greinaert W (1991) Processes accompanying the intrusion of salt lake. In: Breuck WD (ed) *Hydrogeology of salt lake intrusion—a selection of SWIM papers*. Heise, Hannover
- Appelo CAJ, Postma D (1993) *Geochemistry, groundwater and pollution*. Balkema, Rotterdam
- Appelo CAJ, Postma D (2005) *Geochemistry, groundwater and pollution*, 2nd edn. Balkema, Rotterdam
- Barker AP, Newton RJ, Bottrell SH (1998) Processes affecting groundwater chemistry in a zone of saline intrusion into an urban aquifer. *Appl Geochem* 13(6):735–749
- Barlow PM, Reichard EG (2010) Saltwater intrusion in coastal regions of North America. *Hydrogeol J* 18(1):247–260
- Carol E, Kruse E, Mas-Pla J (2009) Hydrochemical and isotopic evidence of groundwater salinization processes on the coastal plain of Samborombon Bay Argentina. *J Hydrol* 365(3):335–345
- Chen CX, Lin M, Zhu WW et al (1993) Groundwater salinization in Yuncheng City predicated by a quasi three dimensional numerical simulation. *Earth Sci* 18(1):48–59
- Craig H (1961) Standards for reporting concentrations of deuterium and oxygen-18 in natural waters. *Science* 133(3467):1833–1834
- Cruz JV, Silva MO (2000) Groundwater salinization in Pico Island (Azores, Portugal): origin and mechanisms. *Environ Geol* 39(10):1181–1189
- Currell MJ, Cartwright I, Bradley DC, Han DM (2010) Recharge history and controls on groundwater quality in the Yuncheng Basin, north China. *J Hydrol* 385(1):216–229
- Datta PS, Tyagi SK (1996) Major ion chemistry of groundwater in Delhi area: chemical weathering processes and groundwater regime. *J Geol Soc India* 47(2):179–188
- Deutsch WJ (1997) *Groundwater geochemistry: fundamentals and application of contamination*. CRC, Boca Raton
- Freeze RA, Cherry JA (1979) *Groundwater*. Prentice-Hall Inc., New Jersey
- Gao XB, Wang YX, Li YL (2007) Enrichment of fluoride in groundwater under the impact of saline water intrusion at the salt lake area of Yuncheng Basin, northern China. *Environ Geol* 53(4):795–803
- Geraghty JJ, Miller DW (1973) *Water atlas of the United States*. Water Information Center, Washington, United States



- Ghabayen S, Mckee M, Kemblowski M (2006) Ionic and isotopic ratios for identification of salinity sources and missing data in the Gaza aquifer. *J Hydrol* 318(1):360–373
- Gibson JJ, Edwards TWD, Burse GG (1993) Estimating evaporation using stable isotopes quantitative results and sensitivity analysis for two catchments in northern Canada. *Nord Hydrol* 24(2):79–94
- Guo HM, Wang YX (2005) Geochemical characteristics of shallow groundwater in Datong Basin, northwestern China. *J Geochem Explor* 87(3):109–120
- Han Y, Yan SL, Ma HT, Zhang HM, Wu JZ, Wang YX, Liang X, Xu HL, Ma T, Tang ZH (2006) Groundwater resources and environmental issues assessment in the six major basins of Shanxi province. Geological Publishing House, Beijing **(in Chinese)**
- Heaton THE (1986) Isotopic studies of nitrogen pollution in the hydrosphere and atmosphere: a review. *Chem Geol* 59(1):87–109
- Houghton JT, Meira Filho LG, Callander N et al (1996) Climate change 1995, the science of climate change. Cambridge University Press, Cambridge
- Huang XX, Dong SG, Tang ZH et al (2007) Groundwater numerical simulation and prediction of Yuncheng Basin. *Resour Environ Eng* 21(4):402–406
- IAEA (1993) Reference and inter-comparison materials for stable isotopes of light elements. In: Proceeding of a consultants meeting held in Vienna, 1–3 1993, IAEA, Vienna, TECDOC-825: 165
- Jalali M (2007) Hydrochemical identification of groundwater resources and their changes under the impacts of human activity in the Chah basin in western Iran. *Environ Monit Assess* 130(1):347–364
- Khair AM, Li CC, Hu QH et al (2014) Fluoride and arsenic hydrogeochemistry of groundwater at Yuncheng Basin, Northern China. *Geochem Int* 52(10):868–881
- Li CC, Gao XB, Wang YX (2015) Hydrogeochemistry of high-fluoride groundwater at Yuncheng Basin, northern China. *Sci Total Environ* 2015(508):155–165
- McMillion LG (1965) Hydrologic aspects of disposal of oil-field brines in Texas. *Groundwater* 3(4):36–42
- Miller MR (1981) Saline seep development and control in the North American Great Plains-Hydrogeological aspects. *Agric Water Manage* 4(1):115–141
- Parkhurst DL, Appelo CAJ (1999) User's guide to PHREEQC (version 2): a computer program for speciation, batch-reaction, one dimensional transport, and inverse geochemical calculations. US Geological Survey Water-Resources Investigations Report, pp 99–4259
- Rouchy JM, Caruso A (2006) The Messinian salinity crisis in the Mediterranean basin: a reassessment of the data and an integrated scenario. *Sed Geol* 188(15):35–67
- Sami K (1992) Recharge mechanisms and geochemical processes in a semi-arid sedimentary basin, Eastern Cape, South Africa. *J Hydrol* 139(1):27–48
- Tanji KK (1990) Nature and extent of agricultural salinity. In: Agricultural salinity assessment and management, American Society of Civil Engineers, New York
- Tellam JH (1995) Hydrochemistry of the saline groundwaters of the lower Mersey Basin Permo-Triassic sandstone aquifer, UK. *J Hydrol* 165(1):45–84
- Trabelsi R, Zairi M, Ben Dhia H (2007) Groundwater salinization of the Sfax superficial aquifer, Tunisia. *Hydrogeol J* 15(7):1341–1355
- Wallender WW, Tanji KK (1996) Agricultural salinity assessment and management. American Society of Civil Engineers, USA
- Wang YX, Shvartsev SL, Su CL (2009) Genesis of arsenic/fluoride-enriched soda water: a case study at Datong, Northern China. *Appl Geochem* 24(4):641–649
- Wang YX, Gao XB, Li CC (2013) Genesis of high F groundwater in Yuncheng Basin, Shanxi Province, northern China (Research project report in Chinese)
- Yang Y, Lu LL (2005) On Yuncheng city's present situation and exiting problems of water resources and its countermeasure. *Shanxi Hydrotech* 3:38–40
- Yuan HT (2003) Development and utilization of saline groundwater in Yuncheng City, China. *Water Resour* 14:21–22
- Yuncheng Regional Water Bureau and Shanxi province Geological Survey (1982) Hydrological and Geological maps and explanations for the Yuncheng region 1:100000. Special Report **(in Chinese)**